ANALYTICAL AND EXPERIMENTAL INVESTIGATIONS INTO STRUCTURAL DAMAGE IDENTIFICATION USING VIBRATION DATA

Somayya Ammanagi[1]
S Venkatesha[2]
C S Manohar[3]
Department of Civil Engineering
Indian Institute of Science
Bangalore-560 012

Abstract

The paper reports on relative performance of inverse eigensensitivity and response function methods for structural damage detection, location and quantification using vibration data. In implementing each of these methods, a validated baseline finite element (FE) model for the structure, in its undamaged state, is assumed to be available. Depending on this, a matrix of sensitivity of structural dynamic characteristics, in frequency or modal domains, to changes in values of structural parameters, is constructed. An inverse procedure, based on pseudoinverse theory of matrices, is subsequently applied to identify structural damages based on observed changes in vibration response of the structure. Issues arising out of mismatch between degrees of freedom of the FE model and number of measured degrees of freedom are dealt with by using alternative model reduction/expansion schemes. Illustrative examples on synthetically and experimentally generated vibration data on cantilever beams and a three-storied building frame are presented.

1.0 Introduction

Methods for experimentally establishing dynamic characteristics of linear vibrating structures, such as, matrix of impulse response functions, complex frequency response functions, or modal characteristics, namely, natural frequencies, modal damping, and mode shapes, are currently well established (Ewins 2000, McConnell 1995). These characteristics depend upon the physical properties of the structure, such as, elastic constants, mass density, boundary conditions, and geometric characteristics. Any modifications to these characteristics imprint their effects on the structural dynamic properties. Any such modification is treated in the present study as a "structural damage". The methods of vibration based structural inspection are based on the premises that (a) these changes are observable, and (b) *via* the application of inverse procedures, these changes can be related to the causative modifications to the physical parameters of the structure. In the present study it is assumed that the scope of this inspection includes the detecting, locating and quantifying the structural damages.

---

[1] Project Assistant
[2] Technical Officer
[3] Associate Professor, Author for correspondence; mailto:manohar@civil.iisc.ernent.in

The problem of damage location and quantification generally requires the availability of a validated finite element (FE) model for the structure in its undamaged state. Such a model is obtained by spatial discretization of a continuum. The highest frequency up to which one can trust the FE model predictions depends upon the fineness of spatial discretization. A FE model with N degrees of freedom, in principle, possesses N natural frequencies but only about the first 10% of these modes possess trustworthy accuracy. Those modes that are essentially trustworthy would be spatially complete. The current state-of-art in FE modeling permits fairly elaborate models for vibrating structures to be constructed even on desktop computers. Experimental models, on the other hand, are often spatially far less complete than corresponding FE models. This is because of limitations on number of channels for vibration measurements, inaccessibility of interior degrees of freedom (dofs) for measurement and inability to measure rotational dofs. The highest frequency up to which an experimental model can be trusted depends upon sampling frequency and anti-aliasing filter characteristics. The current state-of-the art in vibration data acquisition permits fairly large sampling rates in vibration data acquisition, and, consequently, experimental models are modally incomplete to a lesser extent than corresponding FE models. The incompleteness that invariably exists in FE models and experimental models poses fundamental difficulties in terms of non-uniqueness and ill posedness of governing equations in problems of FE model updating (Friswell and Mottershead 1996) and damage identification. The success of damage detection algorithm crucially hinges upon how these difficulties are dealt with. The problem of structural damage detection is also beset with other difficulties such as those arising due to presence of measurement noise, effect of environment (such as temperature and humidity fluctuations, and presence of ambient loads, such as, those caused due to wind), and possibility of damaged structure entering nonlinear regimes. The optimal selection of location of sensors and actuators so as to achieve the best possible results in damage identification, also constitutes a challenging problem. Obtaining vibration signatures from large-scale civil structures is often a difficult task because of limitations in supplying meaningful test signals that produce structural responses whose levels climb over the measurement noise floor. Furthermore, as has been noted already, when damages need to be localized *and* quantified, a validated baseline FE model for the structure, in its undamaged, state would often be required. Fulfilling this requirement may however pose significant difficulties. A systematic treatment of these issues poses several research challenges and, consequently, this subject has received much research attention in the existing literature: the works of Farrar *et al.*, 2001, Doebling *et al.*, 1998, Doebling *et al.*, 1996, He 1999, Salawu 1997, Staszewski 1998, and Farrar *et al.*, 1999, provide comprehensive overviews on the basic research issues in this area. The paper by Majumder and Manohar (2003) contain references to studies on structural damage detection using vibration data for civil engineering structures.

A combined experimental and analytical program of research aimed at developing methods for structural damage detection using vibration data under ambient loads and Bayesian methods for FE model updating is currently underway at the Indian Institute of Science. The work done so far has resulted in the development of a time domain algorithm for damage detection in beams using vibration data generated by a moving

oscillator (Majumder and Manohar 2003,2004). This work has potential applications to damage detection in bridge structures based on measurement of vibration produced by moving vehicles. In the present paper, we report on a comparative study of alternative algorithms for damage detection in linear systems, which are based on frequency and modal domain descriptions. These procedures are applied on synthetically and experimentally generated data. Experimental studies are conducted on cantilever beams and on a three-storied building frame model and this has involved measurement of a set of frequency response functions using impulse hammer tests on the structure in its original state and in a modified state and subsequent extraction of modal parameters using curve fitting methods. The analytical methods of damage identification, when applied to experimental data, are shown to be successful in characterizing structural modifications with reasonable accuracy.

2.0 Basic formulation

The equilibrium equations governing the dynamics of a N degrees-of-freedom linear time invariant system, in time and frequency domains, are respectively given by

$$M\ddot{x}(t) + C\dot{x}(t) + Kx(t) = f(t) \cdots (1)$$

$$[D(\omega)]X(\omega) = F(\omega) \ldots (2)$$

Here M= mass matrix, K= stiffness matrix, C= damping matrix, $D(\omega)=[-\omega^2 M + i\omega C + K]$ is the dynamic stiffness matrix, $x(t)$= $N \times 1$ displacement vector, $f(t)$= $N \times 1$ force vector, $X(\omega)$= Fourier transform of $x(t)$, $F(\omega)$= Fourier transform of $f(t)$, t= time, ω= frequency, i= imaginary number and a dot over head represents derivative with respect to time t. Taking into account the assembling procedure followed in finite element formulation, the structural matrices can be represented in the form

$$M = \sum_{s=1}^{N_e} [A]_s^t [M]_s^e [A]_s \qquad K = \sum_{s=1}^{N_e} [A]_s^t [K]_s^e [A]_s \qquad C = \sum_{s=1}^{N_e} [A]_s^t [C]_s^e [A]_s \cdots\cdots(3)$$

Here the superscript e denotes the element, N_e is the number of finite elements and $[A]_s$ is the nodal connectivity matrix of size $NDOF \times N$ where $NDOF$ is the number dofs in the sth element. An outstanding feature of damage detection problem arises because of the fact that the size of the baseline FE model and the experimental model invariably does not match. This obligates the requirement that, either the FE model must be reduced, or, the experimental model be expanded, so as to achieve a match between the two model sizes. For the purpose of illustration we consider the first option in this discussion. The displacement vector $x(t)$ is partitioned as $x(t)=\{ x_m(t)\ x_s(t) \}^t$ where, superscript t denotes the matrix transpose operation, $x_m(t)$= master dofs of size $N_m \times 1$ that are measured and $x_s(t)$= slave dofs of size $N_s \times 1$ that are not measured. This partitioning automatically induces the following partitioning into the structural matrices

$$M = \begin{bmatrix} M_{mm} & M_{ms} \\ M_{sm} & M_{ss} \end{bmatrix}; C = \begin{bmatrix} C_{mm} & C_{ms} \\ C_{sm} & C_{ss} \end{bmatrix}; K = \begin{bmatrix} K_{mm} & K_{ms} \\ K_{sm} & K_{ss} \end{bmatrix}; D = \begin{bmatrix} D_{mm} & D_{ms} \\ D_{sm} & D_{ss} \end{bmatrix} \cdots (4)$$

Similarly, the force vector $f(t)$ gets partitioned as $f^t=[f_m\, f_s]$. It assumed that the slave dofs are not externally driven and, therefore, it follows that $f_s(t)=0$. Let Φ denote the matrix of modal vectors normalized such that $\Phi^t M \Phi=I$, where I is the identity matrix. This matrix also gets partitioned as $\Phi^t=[\Phi_m\, \Phi_s]$. The master dofs are taken to be related to the displacement vector $x(t)$ through the relation $x=Wx_m$, where, W is the transformation matrix that depends upon the reduction scheme adopted. There exist several reduction schemes in the literature, such as, static and dynamic condensation techniques and system equivalent reduction and expansion process (SEREP), which could be used in this context (Callhan *et al.*, 1989). According to the static condensation technique, this transformation matrix reads

$$W = \begin{bmatrix} I \\ -K_{ss}^{-1} K_{sm} \end{bmatrix} \cdots (5)$$

Similarly, in dynamic condensation one gets,

$$W = \begin{bmatrix} I \\ -[K_{ss} - \omega^2 M_{ss}]^{-1}[K_{sm} - \omega^2 M_{sm}] \end{bmatrix} \cdots (6)$$

According to the system equivalent reduction expansion process (SEREP), the transformation matrix is given by

$$W = \begin{bmatrix} \Phi_m \\ \Phi_s \end{bmatrix} \begin{bmatrix} \Phi_m^t \Phi_m \end{bmatrix}^{-1} \Phi_m^t \cdots (7)$$

Upon substituting equation $x=Wx_m$ in equation (1) and pre-multiplying by W^t one gets

$$M_R \ddot{x}_m + C_R \dot{x}_m + K_R x_m = f_R(t) \cdots (8)$$

Here the quantities $M_R = W^t MW$, $C_R = W^t CW$, and $K_R = W^t KW$ are, respectively, the reduced mass, damping and stiffness matrices and $f_R = W^t f(t)$ is the reduced force vector. In implementing damage detection strategies, the kth element structural matrices are multiplied by non-dimensional damage indication factors α_k, β_k, and γ_k for $k=1,2,...,N_e$ as follows:

$$M_{Dk} = \alpha_k M_{Uk}; C_{Dk} = \beta_k C_{Uk}; K_{Dk} = \gamma_k K_{Uk} \cdots (9)$$

Here the subscript k denotes the element number, and D and $U,$ respectively, denote damaged and undamaged states. Thus, the assembled structural matrices for the damaged structure can be written as

$$M_D = \sum_{k=1}^{N_e} \alpha_k A_k^T M_{Uk} A_k; \quad C_D = \sum_{k=1}^{N_e} \beta_k A_k^T C_{Uk} A_k; \quad K_D = \sum_{k=1}^{N_e} \gamma_k A_k^T K_{Uk} A_k \cdots\cdots(10)$$

The basic problem of damage detection using vibration data can be stated as finding α_k, β_k, γ_k for $k=1,2,...,N_e$, given the difference in response characteristics of the structure in its undamaged and damaged states. These characteristics could be stated in terms of system eigensolutions, matrix of impulse response functions, matrix of frequency response functions, or structural response to given excitations either in time or frequency domains. Depending upon which response characteristic is used in damage detection, and, also based on which reduction scheme is used in FE model reduction, several variants of damage detection algorithms are thus possible. In most situations these algorithms lead to a set of over-determined nonlinear algebraic equations for the damage indicator factors α_k, β_k, γ_k and one needs to employ an iterative scheme combined with the theory of matrix pseudoinverse to obtain the optimal solutions. It may be noted that the relative merits of the above-mentioned reduction schemes are widely discussed in the literature, see, for instance, Callahan *et al*., (1989). The accuracy of static and dynamic condensation techniques is affected by the choice of active dofs. On the other hand, SEREP provides features that the other two reduction schemes do not such as (Callahan *et al*., 1989):

- The arbitrary selection of modes that are to be preserved in the reduced system model.
- The quality of the reduced model is not dependent upon the location of the selected active dof.
- The frequencies and the mode shapes of the reduced system are exactly equal to the frequencies and mode shapes (for the selected modes) of the full system model.

In the present study we consider the use of SEREP and dynamic condensation method for the model reduction.

3.0 Methods of damage detection

3.1 Response function method

Here we consider two structural models representing, respectively, the structure in its undamaged state and damaged state. The governing equations, in frequency domain, for the damaged structure when the system is driven by point harmonic excitations, is given by

$$[-\omega^2 M_D + i\omega C_D + K_D]X_D = F \cdots\cdots(11)$$

Here the subscript U denotes the damaged state. If X_{DR} are the measured dofs, we represent $X_{DR} = W_D X_D$, where W_D is the model reduction transformation matrix for the structure in its damaged state. In the present study we explore the use of two alternative

model; reduction schemes, namely, the SEREP (equation 7) and dynamic condensation (equation 6). Using this transformation, equation (11) can be recast as

$$W_D^T[-\omega^2 M_D + i\omega C_D + K_D]W_D = W_D^T F = F_{DR} \cdots\cdots(12)$$

This can further represented as

$$\begin{bmatrix} [U(\omega)] & [V(\omega)] & [W(\omega)] \end{bmatrix}\begin{Bmatrix} \{\alpha\} \\ \{\beta\} \\ \{\gamma\} \end{Bmatrix} = \{F_D\} \cdots\cdots(13)$$

Here $\{\alpha\} = \{\alpha_k\}_{k=1}^{N_e}, \{\beta\} = \{\beta_k\}_{k=1}^{N_e}, \{\gamma\} = \{\gamma_k\}_{k=1}^{N_e}$ and

$$U_k = -\omega^2 W_D^T A_k^T M_{Uk} A_k W_D X_{DR}$$
$$V_k = -i\omega W_D^T A_k^T C_{Uk} A_k W_D X_{DR}$$
$$W_k = W_D^T A_k^T K_{Uk} A_k W_D X_{DR} \cdots\cdots(14)$$

Equation (13) can be written for $\{\omega\} = \{\omega_s\}_{s=1}^{Q}$, leading to

$$\begin{bmatrix} [U(\omega_1)] & [V(\omega_1)] & [W(\omega_1)] \\ [U(\omega_2)] & [V(\omega_2)] & [W(\omega_2)] \\ \vdots & \vdots & \vdots \\ [U(\omega_Q)] & [U(\omega_Q)] & [U(\omega_Q)] \end{bmatrix}\begin{Bmatrix} \{\alpha\} \\ \{\beta\} \\ \{\gamma\} \end{Bmatrix} = \begin{Bmatrix} F_{DR}(\omega_1) \\ F_{DR}(\omega_2) \\ \vdots \\ F_{DR}(\omega_Q) \end{Bmatrix} \cdots\cdots(15)$$

This equation can be written compactly as

$$[\Omega]\{\delta\} = \overline{F} \cdots\cdots(16)$$

It may be noted that the coefficient matrix *[Ω]* here is complex valued. In the solution of the above equation, it is found expedient to separate the real and imaginary parts of *Ω* and F as *[Ω]=R+iI* and *F=G+iH* . Consequently, equation (23) can be recast as

$$\begin{bmatrix} R \\ I \end{bmatrix}\{\delta\} = \begin{Bmatrix} G \\ H \end{Bmatrix} \cdots\cdots(17)$$

It is important to note that the quantities *R, I, G* and *H* are functions of W_D, and, hence, are functions of the unknown vector *δ*. Thus equation (17) represents a set of nonlinear equations in *δ*. In the present study, we adopt an iterative strategy to solve these equations. Towards this end, we begin by assuming that $W_D=W_U$. With this assumption, the governing equation for *δ* becomes linear in nature. In most applications these equations constitute a set of over-determined set of linear algebraic equations with the

number of equations exceeding the number of unknowns. An optimal solution to the damage indicator factor δ can be obtained using pseudo-inverse theory as

$$\{\delta\} = \begin{bmatrix} R \\ I \end{bmatrix}^+ \begin{Bmatrix} G \\ H \end{Bmatrix} \cdots\cdots (18)$$

Here the superscript + denotes the pseudo-inverse defined for a rectangular matrix A by $A^+ = [A^t A]^{-1} A^t$. With this initial value of δ, an updated estimate of W_D is constructed and the iterative process is repeated till satisfactory convergence on δ is achieved. The knowledge of this damage indication vector enables the definition of element location and quantification of the structural damages.

3.2 Inverse eigensensitivity method

Methods for evaluating sensitivity of natural frequencies and mode shapes of vibrating systems with respect to system parameters is a widely studied subject; one of the early papers in this area has been by Fox and Kapoor (1968). These methods prove to be valuable in formulating problems of linear structural damage detection using vibration data. Here one constructs a matrix of sensitivity factors of natural frequencies and mode shapes with respect to structural parameters that are linked with damage indicator factors. This information is subsequently used in relating the observed differences in eigensolutions of the structure, in its undamaged and damaged states, to the physical location and severity of the structural damage.

Let $\{\delta\}$ be the l-dimensional vector of structural parameters, which can change due to occurrence of damage. Let the jth element of this vector be δ_{j0} in the undamaged state and, in the damaged state, let this parameter change to $\delta_{j0} + \Delta\delta_j$. Consider the rth eigenvalue λ_r and the rth eigenvector $\{X_r\}$ and let $\Delta\lambda_r$ and ΔX_r, respectively, denote the changes in λ_r and $\{X_r\}$ caused due to the damage. Using first order Taylor's expansion one can write

$$\Delta\lambda_r \cong \sum_{j=1}^{l} \Delta\delta_j \frac{\partial \lambda_r}{\partial \delta_j}(\delta_0)$$

$$\Delta X_r \cong \sum_{j=1}^{l} \Delta\delta_j \frac{\partial X_r}{\partial \delta_j}(\delta_0) \cdots\cdots (19)$$

If the gradients of eigensolutions with respect to δ_j are available, then, the above equations can re-cast schematically as

$$\{\Delta\upsilon\} = [S]\{\Delta\delta\} \cdots\cdots (20)$$

Here $\Delta\upsilon$ is the vector of difference in eigensolutions of the structure in its damaged and undamaged states, S is the matrix of sensitivity factors and $\Delta\delta$ is the correction factor. This equation typically constitutes a set of over-determined linear algebraic equations in

$\Delta\delta$ and an optimal solution is obtained as $\Delta\delta=[S]^+\{\Delta v\}$. It can be shown that (Fox and Kapoor 1968)

$$\frac{\partial \lambda_i}{\partial \delta_j} = X_i^t\left[\frac{\partial K}{\partial \delta_j} - \lambda_i \frac{\partial M}{\partial \delta_j}\right]X_i \cdots\cdots(21)$$

$$\left\{\frac{\partial X_i}{\partial \delta_j}\right\} = \begin{bmatrix} F_i \\ 2X_i^t M \\ 2X_i^t M \end{bmatrix}^+ \left\{\begin{matrix} 0 \\ 0 \\ \frac{\partial \lambda_i}{\partial \delta_j} \end{matrix}\right\} - \begin{bmatrix} F_i \\ 2X_i^t M \\ 2X_i^t K \end{bmatrix}^+ \begin{bmatrix} \frac{\partial F_i}{\partial \delta} \\ X_i^t \frac{\partial M}{\partial \delta_j} \\ X_i^t \frac{\partial K}{\partial \delta_j} \end{bmatrix}\{X_i\} \cdots\cdots(22)$$

If δ_j is interpreted as damage indicator factor, the derivative of the K and M matrices can easily be evaluated by using equation (3). It must be noted that in deriving these sensitivities it is assumed that no model reduction has been done in obtaining mass and stiffness matrices. In case model reduction is indeed implemented, the mass and stiffness matrices appearing in equations (21) and (22) need to be interpreted as the reduced mass and stiffness matrices. In this case, additional information on derivative of reduced structural matrices with respect to δ_j would be needed. For complicated structures such information may not be easily available. This is particularly true when the structure under consideration is modeled using commercially available FE codes, which often do not have capability to report on eigensensitivity vectors. In such cases, the eigensensitivity vectors can be estimated numerically. This involves repeated runs of the FE codes for a matrix of values of design parameter δ followed by numerical differentiation of the desired response quantity with respect to the structural variable of interest. This enables the estimation of the sensitivity matrix *[S]* appearing in equation (20) and hence an approximate solution to the problem on hand.

Remarks

1. The frequency domain method employs the SEREP for analytical model reduction and, given the iterative strategy adopted in the study, the proposed method does not need a modal analysis to be done on the experimental model of the damaged structure. The SEREP used is a high fidelity reduction scheme, which retains features of original model in both modal and spatial domains. In implementing this method, the number of equations to be used and the choice of frequencies at which these equations are formulated are crucial to the success of the method. The error of optimally solving the over-determined equations offers a means to make this decision. The method has the potential for updation of the damping matrix. However, the model reduction scheme employed here does not include the effect of damping matrix. This can be remedied if one includes the effect of damping in the definition of *W* in carrying out the SEREP.

2. The inverse eigensensitivity methods require that an experimental modal analysis be performed on the damaged structure. The method handles relatively less amount of information as compared to the response function method. Furthermore, the sensitivity of the reduced models needs to be related to the parameters of the original model. Here again, SEREP appears to be the best choice for reducing the model. The method, in its present form, is inherently incapable of detecting changes to the damping characteristics caused due to damage.

3. Both these methods, used in conjunction with numerical methods for sensitivity computations, have the promise of being applicable to large scale structures wherein it is expedient to use commercially available FE codes for modeling and when the FE codes used do not have capability to provide the required eigensensitivity information.

4. In the methods discussed herein it is assumed that a larger FE model is reduced to match the size of the smaller experimental model. An alternative to this would be to retain FE model untouched but instead resort to expanding the experimental model using additional information from the analytical model.

5. The tools such as, modal assurance criterion (MAC) and coordinate modal assurance criterion (COMAC) (Ewins 2000), for comparing two distinct models for eigenvectors, obtained by alternative routes (for example, theoretical & experimental models or models before and after the occurrence of damage), become useful in the context of damage identification. The MAC and COMAC are defined, respectively, by

$$MAC(A,X) = \frac{|\sum_{j=1}^{n} (\psi_X)_j (\psi_A)_j^*|^2}{\left[\sum_{j=1}^{n} (\psi_X)_j (\psi_X)_j^*\right]\left[\sum_{j=1}^{n} (\psi_A)_j (\psi_A)_j^*\right]}$$

$$COMAC(i) = \frac{\sum_{l=1}^{L} |(\psi_X)_{il} (\psi_A)_{il}|^2}{\sum_{l=1}^{L} (\psi_X)_{il}^2 \sum_{l=1}^{L} (\psi_A)_{il}^2}$$

...(23)

Here, ψ denotes the mode shape, the subscripts X and A, respectively, denote the experimental and analytical models. MAC is a scalar quantity defined with respect to a pair of modes, and, when these modes are well correlated, MAC would be close to one. On the other hand, the COMAC is defined with respect to a set of L correlated mode shapes and is a function of the spatial coordinates. If there exists no discrepancies between the two models, the COMAC would be unity. A plot of COMAC between baseline model of the structure, in its undamaged state, and the structure, in its damaged state, is expected to show differences in regions where the effect of damages is felt most pronouncedly; these regions, however, need not correspond to the actual location of damages.

4.0 <u>Illustrations using synthetic vibration data</u>

The problem of validating the algorithms developed for damage detection is considered first. For this purpose, we consider a set of spring supported cantilever beams in which structural modifications are artificially made and the vibration data for damage detection are generated synthetically using finite element method. These studies are meant to be the precursors to the experimental studies to follow on cantilever beams as shown in figure 1. The rotary spring at the end was introduced to cater for the lack of perfect fixity that was found to exist in the experimental model. The parameter τ is used to denote the change in the value of this spring in baseline FE model updating and structural damage detection. The FE model in this study has been created on a Matlab platform. The beam, in its undamaged state, is assumed to have the following properties: L=0.72 m, E=2.0e11 N/m^2, mass density ρ=7528.9 kg/m^3, rectangular cross section with dimensions of 50.6 by 6.4 mm. For the purpose of vibration analysis, the beam is divided into 60 two-dimensional Euler-Bernoulli beam elements. For the purpose of damage identification, the beam is divided into n_s segments; the finite elements lying within each of this segment are assigned a set of common damage indicator factors. In the numerical studies n_s =4 and 6 were considered. Thus, in artificially simulating damage, the flexural rigidity or the mass per unit length of all the elements lying within a segment is changed simultaneously. To start with, vibration data measured from the undamaged structure was inputted to the damage detection algorithms. It was found that the algorithms correctly reported that all the damage indicator factors were unity with an accuracy of higher than 0.001%. Results on damage identification with a distributed scenario of damages using different versions of damage detection methods with different choices for the parameters of the algorithm are summarized in Table 1. An entry denoted by a * in this table indicates the lack of convergence of the detection algorithms for the specific choices of the parameters of the method. The factors that influence the accuracy of damage detection for different methods are summarized below:

   (a) Response function method with model reduction using dynamic condensation: number of master dofs, location of master dofs, location of the driving point, frequency points at which equation (15) is formulated, the location of these frequencies, and number of frequency response functions (FRFs) used in formulating the equations.
   (b) Response function method using SEREP for model reduction: number of master dofs, their location, location of the driving point, number of modes retained in the reduction, the modes that are included, number of frequency points and their location and the number of FRFs used.
   (c) Method based on inverse eigensensitivity: number of measurement points and their location, and number of natural frequencies and mode shapes included in the analysis.

In all these methods, the number of segments n_s into which the beam is divided for the purpose of damage detection also is an important factor. Based on the numerical studies conducted the following observations are made:

(i)   The treatment of rotational dofs as slaves does not affect the success of the damage detection algorithms.

(ii)   In the response function method, with fewer translation dofs treated as masters, the accuracy of the method deteriorates; in some instances, the algorithms failed to converge. The method based on inverse eigensensitivity showed convergent behavior but with increasing errors with reduction in number of masters. In fact with only one master and with information on six eigenvalues, the method converged and could detect damages with accuracy varying from 0.38% to 11.7% depending upon the specific choice of the master dof made.

(iii)   The response function method using dynamic condensation was found to be computationally more intensive as compared with the method based on SEREP. When only four masters were selected, the method based on SEREP failed to provide convergent solutions while the method based on dynamic condensation continued to perform well.

(iv)   In the response function method, with dynamic condensation for model reduction, the set of discrete frequencies that are included in the analysis plays a crucial role. The accuracy does not necessarily improve, as this set is made large. The inclusion of about three frequencies around each resonant peak was found to lead to acceptable convergent behavior of the damage detection algorithm. A similar observation has been made in the existing literature by Rad (1997) in the context of FE model updating.

(v)   The method based on inverse eigensensitivity was found to be the most robust among the three methods studied with respect to variations in number of masters, choices of master dofs and number of segments made for damage detection.

(vi)   The number of iteration cycles, when convergent solutions were possible, varied from about 3 to 4 for the inverse eigensensitivity method and up to about 15 iterations for the response function method.

5.0 Experimental studies

5.1 Studies on cantilever beams

The experimental set up consists of a steel beam 0.72 m long, of rectangular cross-section (50.6 by 6.4 mm) and bolted to a heavy cast iron block at one end (figure 1). The Young's modulus was found to be 2.0e+11 N/m^2 and mass density of 7528.9 kg/m^3. In the analytical model development the beam was divided into 60 finite elements of equal length with a rotary spring inserted at the clamped end to model any lack of fixity against rotation. For the purpose of damage detection, the beam was divided into *6* segments and all the finite elements lying within a segment were assigned the same properties. Thus the spatial resolution of the damage detection in this case is equal to 1/ *6th* of the beam span. For the rotary spring at the end a preliminary value of K_θ=10000 Nm/rad was assigned. An updating exercise based on the method of inverse eigensensitivity was conducted and the results are summarized in Tables 2 and 3. Table 2 shows the summary of results on natural frequencies of the baseline model before and after updating, the experimentally measured natural frequencies on damaged and undamaged beams and the natural frequencies predicted after damage detection was completed. The updating and damage

detection were based on method of inverse eigensensitivity with first six natural frequencies and mode shapes. It may be noted that for the purpose of simulation of a "damage" a concentrated mass of 0.027 kg was placed at a distance of 0.32 m from the support. It was found that the accuracy with which the damage was identified was dependent on the scheme adopted for placement of sensors (figure 1 and Table 4). As can be observed from the results presented in Table 4, the damage detection algorithm locates this mass with accuracy varying from about 0.15% to 5 % depending upon the sensor location scheme. Thus, for scheme 3 the highest error was found to be less than 1.6%. It may be noted that the results shown in Tables 2,3,5 and 6 and 4 correspond to scheme III of sensor placement. It is of importance note in this context that analyses using synthetic data on this system provided equally acceptable results for all the three schemes of sensor placements. Table 5 summarizes the MAC values between experimental observations on damaged and undamaged structures; the values of the natural frequencies and modal damping are also provided here for ready reference. The success of the baseline model updation as well as damage detection can be discerned from COMAC values summarized in Table 6 in which it can be seen that the COMAC value is close to unity at all the dofs. Figure 4 illustrates the experimentally measured and analytically predicted 3rd mode shape for the damaged beam. The close agreement found between these plots again points towards the success of the damage detection process.

In the experimental work the FRFs were measured by using impulse hammer tests. In order to achieve acceptable quality of input pulse, it was found advantageous to select near the beam support to impart the hammer blows. For this purpose the B&K hammer type 8202 with plastic tip, B&K 8200 force transducer and B&K 2635 charge amplifier was used. The acceleration response of the beam was measured at a set of six points by using strain gauge based Sensotech accelerometers. The data was acquired using a PC based, 4-channel 100kHz IOTECH DAQ Board/2000 data acquisition system equipped with an anti-aliasing filter (with cut-off frequency of 1000 Hz) and a simultaneous sampling and hold board. A sampling rate of 4000/s was used in conjunction with a rectangular window (of width 0.05 s) for the hammer blow and an exponential window $[w(t)=exp(-t/0.659)]$ for the beam responses. In Each measurement data of duration 8.192 s was acquired. The FRFs were averaged over 30 samples. A worksheet to conduct the experiment was created on a DASYLab platform. The extraction of modal information from the measured vector of FRFs was carried using the ME'scope software using polynomial curve fitting method with due correction being made for the artificial attenuation effect arising due to the use of exponential window. It may be noted that each of the accelerometers used had a mass of 0.012 kg and these masses were added to the FE model developed for the purpose of damage detection.

5.2 Studies on a three-storied building frame model

Figure 5 shows the model of a three storied, single bay building frame. The columns were made flexible in one direction and slabs were heavier and much more rigid than the columns: this ensured that the structure would behave predominantly as a three-dof shear beam. A three-dof model for the frame was thus made and updated using experimentally measured eigenparameters in conjunction with the inverse eigensensitivity method of

updating. A modification to the structure was artificially simulated by adding a mass of 0.233 kg to the second floor. Table 7 summarizes the results on natural frequencies for the initial assumed model, experimental results on damaged structure, updated baseline model and the predicted values from damaged structure after damage has been analytically detected. Tables 8 and 9 summarize the results on baseline model updating and detection of damage in the modified structure. The results on MAC and COMAC are summarized for the cases of updating of baseline model and for assessment of efficacy of damage detection. As can be observed from Table 9, the damage detection here has been possible with the highest error being less than 3%. The measurement of eigenparameters of the system was based on impulse hammer method and the details of the measurement strategy used was broadly similar to the one followed for the beam structure.

6.0 Closing remarks

The problem of structural damage identification using vibration data in cantilever beam structures and a three-storied shear-building frame is considered. Methods based on FE model updating are employed to detect, locate and quantify the damages. This has involved the application of response function and inverse eigensensitivity methods for element level location and quantification of structural damages. The governing equations for the damage indication factors in both of these methods are shown to constitute a set of over determined coupled nonlinear equations. The nonlinear nature of these equations essentially arises due to the spatial incompleteness of the experimental data. These equations are solved using an iterative strategy. The study has involved both synthetic and experimentally produced data. The studies on using synthetic data have proved to be useful in investigating the range of validity of the damage identification schemes *vis-à-vis* the choices made on number of masters and their location, number of modes retained in the reduced models obtained using SEREP, and number and location of frequency points in reduction method involving dynamic condensation. The convergence and accuracy of the iterative strategy used in damage identification are shown to be dependent on these choices. Additionally, in the studies involving experimental data, the accuracy of damage identification is observed to be strongly influenced by the location of sensors and the drive point. For a given structural damage configuration, analyses using synthetic data provided equally acceptable results for alternative schemes of sensor placement while the damage identification using experimental studies showed significantly varying error patterns. Further studies are needed to explain these patterns of errors observed in damage identification using experimental data. Similarly, the scope of the present study needs to be expanded to include the treatment of measurement noise, more general forms of structural modification due to occurrence of damage (such as, loss of stiffness, changes in damping and/or onset of nonlinear behavior).

References

1. J O Callahan, P Avitable, and R Riemer, 1989, System equivalent reduction expansion process (SEREP), Proceedings of the 7th International Modal Analysis Conference, Las Vegas, Nevada, February, 29-37.
2. S W Doebling, C R Farrar, M B Prime, D W Shevitz, 1996, Damage identification and health monitoring of structural and mechanical systems from changes in their vibration characteristics; A literature review, Los Alamos LA-13070-MS, UC-900, Los Alamos National Laboratory.
3. S W Doebling, C R Farrar, M B Prime, 1998, A summary Review of vibration-based damage identification methods, Shock and Vibration Digest, 30(2), 91-105.
4. D J Ewins, Modal testing: Theory, Practice and Application, Research studies press limited. Baldock, Hertfordshire 2000.
5. C R Farrar, W Scott, S W Doebling, A N David, 2001, Vibration-based structural damage identification, Philosophical Transactions of Royal Society, London, 359, 131 149.
6. C R Farrar, S W Doebling, 1999, Damage detection and evaluation II, A chapter in Modal analysis and Testing, J M M Silva and N M M Maia (Eds.), Kluwer Academic Publishers, Dordrecht, 345-378.
7. R L Fox and M P Kapoor, 1968, Rates of change of eigenvalues and eigenvectors, AIAA Journal, 6, 2426-2429.
8. M I Friswell and J E Mottershead, 1996, Finite element model updating in structural dynamics, Kluwer Academic Publishers, Dordrecht.
9. J He, 1999, Damage detection and evaluation I, A chapter in Modal analysis and Testing, J M M Silva and N M M Maia (Eds.), Kluwer Academic Publishers, Dordrecht, 325-344.
10. K G McConnel, 1995, Vibration testing: theory and practice, John Wiley, New York.
11. L Majumder and C S Manohar, 2003, A time domain approach for damage detection in beam structures using vibration data with a moving oscillator as an excitation source, Journal of Sound and Vibration, 268, 699-716.
12. L Majumder and C S Manohar, 2004, Nonlinear reduced models for beam damage detection using data on moving oscillator-beam interactions, Computers and Structures, 82(2-3), 301-314.
13. S Z Rad, 1997, Methods for updating numerical models in structural dynamics, PhD thesis, Imperial College of Science, Technology and Medicine, University of London.
14. S Salawu, 1997, Detection of structural damage through changes in frequency: a review, Engineering Structures, 19(9), 718-723.
15. W J Staszewski, 1998, Structural and mechanical damage detection using wavelets, The Shock and Vibration Digest, 30(6), 457-472.

Table1 Damage detection in cantilever beams using synthetic vibration data; note: cases for which the damage detection algorithm did not converge is marked by a *.

		IES method	RFM (SEREP condensation)	RFM (Dynamic condensation)
No. of masters	No. of modes	Maximum % error		
6(A1-A6)	6	0.00	0.010	2.47
6(A1-A6)	5	0.00	0.000	0.72
6(A1-A6)	4	0.00	*	7.45
6(A1-A6)	3	0.00	*	12.42
5(A1,A2, A4-A6)	6	0.00	*	0.27
5(A1,A2, A4-A6)	5	0.00	0.01	1.50
4 (A1-A4)	6	0.00	*	0.53
3(A1-A3)	6	0.00	*	0.83
2 (A1-A2)	6	0.00	*	2.01
1 (A1)	6	11.70	*	*
1(A2)	6	11.96	*	*
1(A3)	6	2.40	*	*
1(A4)	6	0.38	*	*

Number of segments for damage detection = 6;
Accelerometer locations as per Scheme 1;
Induced damage: α, β = {0.9,1,0.8,1,0.95,1} and τ = 1.20

Number of segments for damage detection= 4
Accelerometer locations as per Scheme 4;
Induced damage: α,β = {0.9,1,0.8,1} and τ = 1.20

4(A1-A4)	6(1-6)	0.00	*	17.20
4(A1-A4)	5(1-5)	0.00	*	18.34
4(A1-A4)	4(1-4)	0.00	0.00	0.71
4(A1-A4)	3(1-3)	0.00	*	2.17

Table 2 Natural frequencies in Hz for the beam structure.

	Mode 1	Mode 2	Mode 3	Mode 4	Mode 5	Mode 6
Baseline model before updating	9.3891	59.1583	166.4382	326.1528	543.3913	812.7730
Experimental results on undamaged beam	9.3852	59.1470	166.4300	325.3400	539.6300	806.9900
Baseline model after updating	9.3852	59.1470	166.4300	325.3400	539.6300	806.9900
Experimental results on damaged beam	9.3633	58.2770	165.9900	322.0700	536.4100	802.2500
Results predicted after damage detection	9.3633	58.2770	165.9900	322.0700	536.4100	802.2500

Table 3 Updating of baseline model for the beam structure.

Updating parameters	Value before updating	Value after updating	% updation
K_θ (Nm/rad)	10000	12779	-27.7860
M_1 (kg)	0.3643	0.4052	-5.4564
M_2 (kg)	0.2914	0.2821	1.6228
M_3 (kg)	0.2429	0.2449	-0.4155
M_4 (kg)	0.3643	0.4042	-5.3280
M_5 (kg)	0.2429	0.2397	0.6490
M_6 (kg)	0.2429	0.2621	-3.8759

Table 4 Results of damage identification on the beam structure.

Damage indicating parameters	Scheme I			Scheme II			Scheme III		
	Expected vector	Detected vector	% Error	Expected vector	Detected vector	% Error	Expected vector	Detected vector	% Error
A_1	1.0000	1.0093	0.9289	1.0000	0.9668	3.3213	1.0000	0.9915	0.8468
A_2	1.0000	0.9981	0.1916	1.0000	0.9813	1.8734	1.0000	1.0016	0.1586
A_3	1.0732	1.0858	1.1709	1.0824	1.1217	3.6307	1.1153	1.1331	1.5962
A_4	1.0000	0.9519	4.8090	1.0000	0.9954	0.4637	1.0000	0.9887	1.1299
A_5	1.0000	0.9971	0.2865	1.0000	1.0499	4.9947	1.0000	1.0148	1.4836
A_6	1.0000	1.0076	0.7625	1.0000	0.9643	3.5671	1.0000	0.9936	0.6375

Table 5 Details of natural frequencies, modal damping and MAC for experimental measurements on damaged and undamaged structures

Shape			Shape 1	Shape 2	Shape 3	Shape 4	Shape 5	Shape 6
	Frequency (Hz)		9.36329	58.2769	165.994	322.072	536.414	802.25
		Damping (%)	2.81648	0.548626	0.209632	0.160718	0.19635	0.128035
Shape 1	9.38522	2.80894	1.000	0.078	0.076	0.040	0.018	0.031
Shape 2	59.1468	0.570366	0.084	1.000	0.039	0.043	0.125	0.069
Shape 3	166.432	0.213244	0.078	0.030	1.000	0.105	0.108	0.084
Shape 4	325.34	0.155086	0.043	0.030	0.108	0.999	0.078	0.018
Shape 5	539.634	0.195323	0.017	0.130	0.098	0.066	0.999	0.080
Shape 6	806.989	0.116466	0.029	0.076	0.081	0.013	0.089	0.998

Table 6 Details of *COMAC(i)* for baseline model updating and for verifying the efficacy of damage detection. Case 1: updation of baseline model; A= updated analytical model and X= experimental model on undamaged structure. Case 2: check after damage detection; A: analytical model after damages have been identified and X: experimental measurements on damaged structure.

$i \rightarrow$	1	2	3	4	5	6
Case 1	0.9995	0.9892	0.9962	0.9938	0.9930	0.9867
Case 2	0.9993	0.9903	0.9961	0.9933	0.9915	0.9894

Table 7 Natural frequencies in Hz for the frame structure.

	Mode 1	Mode 2	Mode 3
Baseline model before updating	2.8495	7.9650	11.4742
Experimental results on undamaged frame	2.7931	7.9084	11.6370
Results from the updated baseline model	2.7931	7.9084	11.6370
Experimental results on damaged frame	2.7306	7.8676	11.2670
Results predicted after damage detection	2.7306	7.8676	11.2670

Table 8 Updating of the baseline model for the frame structure.

Updating parameters	Value before updating	Value after updating	% updation
M_1 (kg)	1.9430	1.8846	3.0063
M_2 (kg)	1.9430	1.8449	5.0510
M_3 (kg)	1.8938	2.1107	-11.4544

Table 9 Results on the damage detection for the frame structure.

Damage indicating parameters	Expected vector	Detected vector	% Error
α_1	1.0000	0.9802	1.9847
α_2	1.1182	1.1508	-2.9132
α_3	1.0000	0.9999	0.0094

Table 10 Details of natural frequencies, modal damping and MAC for experimental measurements on damaged and undamaged structures

Shape			Shape 1	Shape 2	Shape 3
	Frequency (Hz)		2.7306	7.8676	11.267
		Damping (%)	2.5134	0.92839	0.68966
Shape 1	2.7931	2.43	0.999	0.005	0.003
Shape 2	7.9084	0.92567	0.005	0.999	0.001
Shape 3	11.637	0.67473	0.000	0.008	0.995

Table 11 Details of *COMAC(i)* for baseline model updating and for verifying the efficacy of damage detection. Case 1: updating of baseline model; A= updated analytical model and X= experimental model on undamaged structure. Case 2: check after damage detection; A: analytical model after damages have been identified and X: experimental measurements on damaged structure.

$i\rightarrow$	1	2	3
Case 1	0.9986	0.9917	0.9863
Case 2	0.9956	0.9866	0.9874
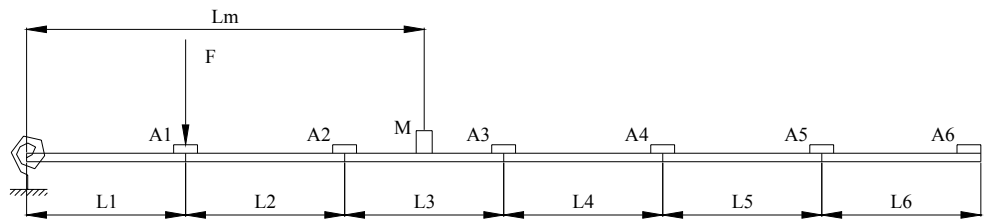
A1-A6: Accelerometers

F: Excitation (Impulse hammer)
M: Mass (Structural modification)
Kt: Torsion spring

SCHEME	L1	L2	L3	L4	L5	L6	Lm
1	120	120	160	80	120	120	320
2	140	110	140	110	110	110	320
3	150	120	100	150	100	100	320
4	200	200	160	160	-	-	-

All dimensions in mm

Figure 1 Details of experimental setup for studies on cantilever beam.
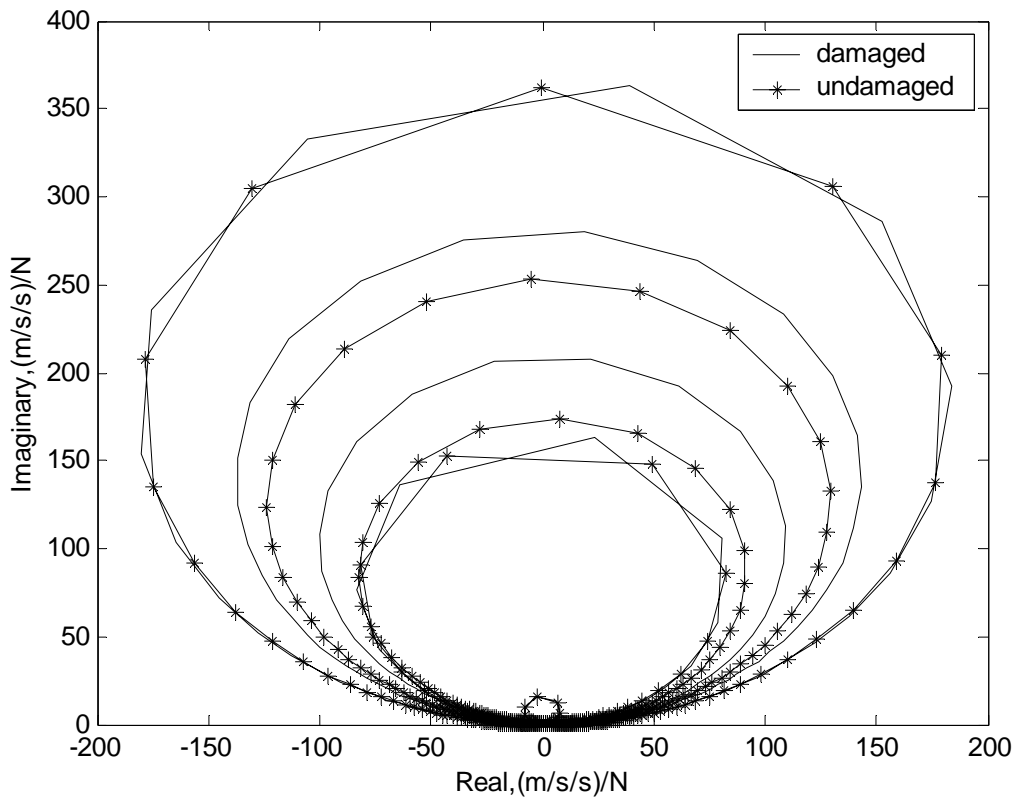
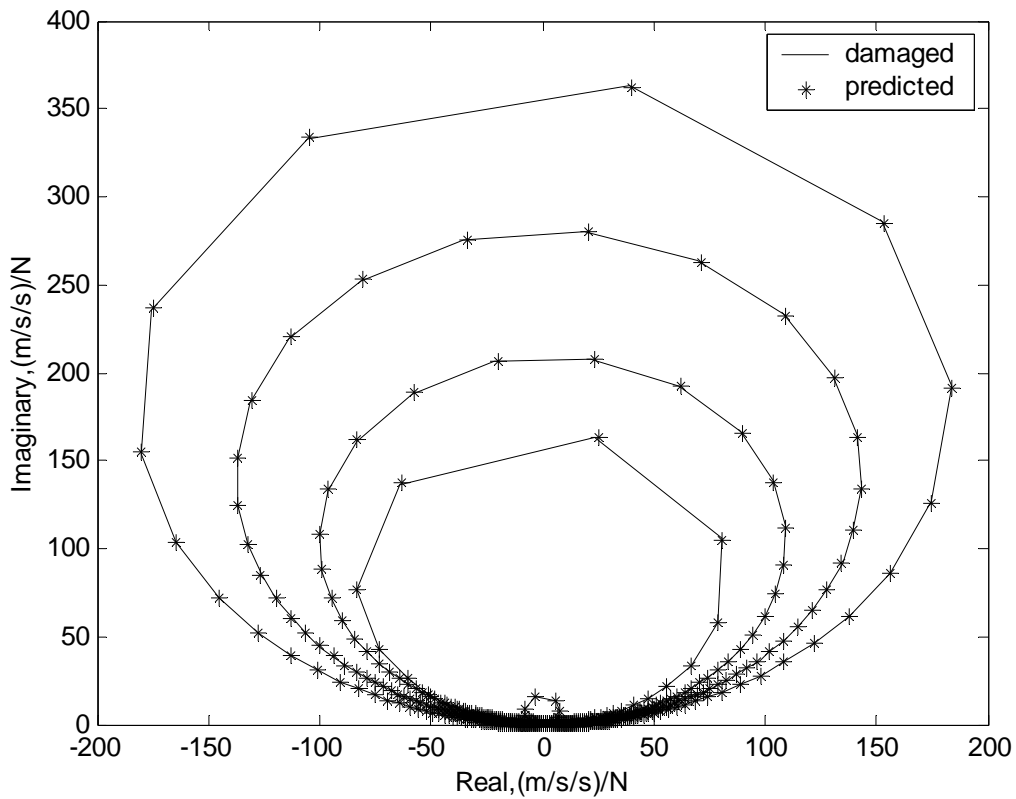Figure 2 Point FRF of beam in undamaged and damaged states

Figure 3 Analytical FRF of the damaged beam and the FRF predicted from the baseline model after damage detection.
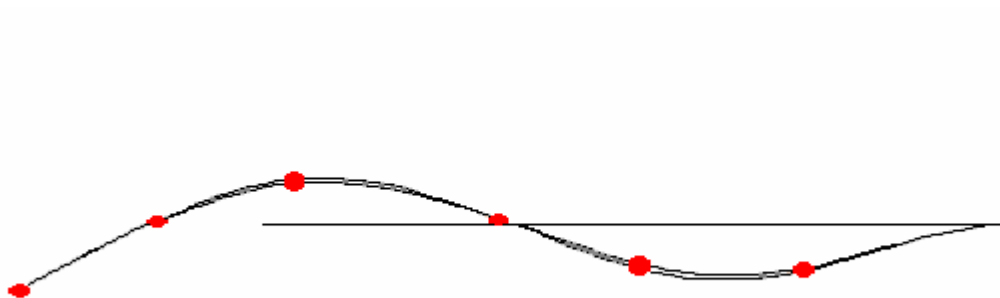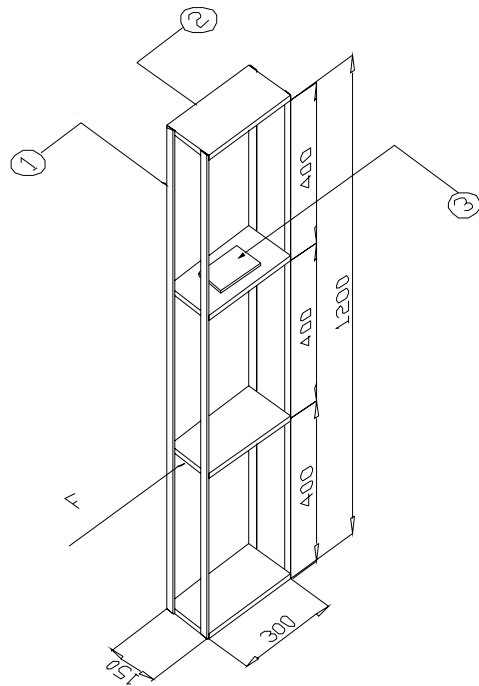

Figure 4. Comparison of 3rd mode shape for the damaged beam obtained using experiments and predicted using detected damage parameters; the dots represent points at which measurements are made.

Part no.	Part Description	Numbers	Size (mm)
1	Column	4	3x25x1200
2	Slab	4	12.5x150x300
3	Plate	1	7x85x140

$E=69e9 \text{ N/m}^2$, $\rho=2800 \text{ kg/m}^3$

Figure 5 Model of a 3-story building; F: force applied.